Fiber-coupled semiconductor waveguides as an efficient optical interface to a single quantum dipole

Marcelo Davanço[*1,2] and Kartik Srinivasan[1]

[1]*Center for Nanoscale Science and Technology, National Institute of Standards and Technology, Gaithersburg, MD* [2]*Maryland NanoCenter, University of Maryland, College Park, MD, 20742*
[*]*Corresponding author: mdavanco@nist.gov*

We theoretically investigate the interaction of a single quantum dipole with the modes of a fiber-coupled semiconductor waveguide. Through a combination of tight modal confinement and phase-matched evanescent coupling, we predict that ≈ 70 % of the dipole's emission can be collected into a single mode optical fiber. We further show that the dipole strongly modifies resonant light transmission through the system, with over an order of magnitude change for an appropriate choice of fiber-waveguide coupler geometry. © 2009 Optical Society of America

OCIS codes: 350.4238, 270.0270

The interaction of a single quantum dipole with a strongly confined optical field is a central paradigm in quantum optics [1]. The ability to collect a large fraction of the dipole's emission or use it to modify an incident optical field lies behind a number of proposed applications in areas such as classical and quantum information processing [1–5] and single emitter spectroscopy [6]. Such applications depend on the availability of efficient and accessible dipole excitation and emission channels. For instance, a single atom in free-space is exclusively excited by the dipole wave component of an illuminating field [2], and perfect reflection of an illuminating directional dipolar field is expected [7]. Alternately, a single atom inside a Fabry-Perot cavity is strongly excited by, and radiates efficiently into, externally-accessible cavity modes and profoundly modifies the resonator transfer function [1]. Here, we theoretically investigate a system in which a single emitter embedded in a fiber-coupled semiconductor channel waveguide is optically accessed with high efficiency, potentially yielding > 70 % fluorescence collection into a single mode optical fiber. When resonantly interrogated, the dipole modifies the system's transmission level by over an order of magnitude (≈ 15 dB).

Our system (Fig. 1) is an emitter embedded in a suspended semiconductor channel waveguide (WG), evanescently coupled to an optical fiber taper WG. The taper is a single mode optical fiber whose diameter has been adiabatically and symmetrically reduced to a wavelength-scale minimum, resulting in a low-loss, double-ended device with standard fiber input and output. Fiber and channel WGs form a directional coupler (cross-section shown in Fig. 1(a)) of length L_c, so power may be transferred between the two guides. This system serves as an efficient optical interface to a single dipole due to the availability of a small number of WG modes with highly effective coupling to the atomic transition (i.e., high β-factors [8,9]), and access to such modes via the fiber taper WG, which links on-chip nanophotonics and off-chip fiber optics. As depicted in Fig. 1(c), a signal launched into the fiber input, adiabatically reduced in size along the fiber taper, excites supermodes of the directional coupler. Guided supermodes illuminate the WG-embedded dipole at position z_0 along the coupler. Upon non-resonant excitation, the dipole emits coupler supermodes, at a red-shifted wavelength, in the $\pm z$ directions [10]. Emitted supermodes are converted into input and output fiber modes through the taper transition regions, after which emission is detected. The individual supermode contribution to the total photoluminescence (PL) collection efficiency, η_{PL}, is $\eta_{\mathrm{PL},m} = f_m \cdot \Gamma_m/\Gamma = f_m \cdot \gamma_m$, where Γ_m is the supermode emission rate, and Γ the total emission rate [11]. The fraction γ_m is supermode m's β-factor. Since emission in both $\pm z$ directions is equally likely, $0 \leq \gamma_m \leq 0.5$. The fiber mode fraction, f_m, is an overlap integral between the fundamental fiber mode and supermode m [11, 12]. Its quantum mechanical operator analog is given here as Eq. (2).

We study a geometry modeling a suspended GaAs channel with an embedded self-assembled InAs quantum dot(modeled as a two-level atom with electric dipole moment on the xz plane) produced from the material used in [13]. The channel WG, surrounded by air, has thickness $t_{\mathrm{ch}} = 256\,\mathrm{nm}$, width W_{ch}, and refractive index $n=3.406$ at a wavelength $\lambda = 1.3\,\mu\mathrm{m}$. The adjacent fiber has a 500 nm radius and $n=1.45$. For our parameter range, the directional coupler region supports a set of propagating supermodes named $\mathrm{hE}_{11}^{x,y}$, hybrids of the $\mathrm{E}_{11}^{x,y}$ rectangular dielectric channel WG modes [14] and fundamental fiber mode. Supermodes hE_{11}^x and hE_{11}^y are excited by the x- and z-electric dipole moment components, respectively. Following [11], where fiber-based collection of emitters in membranes was studied, supermode field profiles (calculated with the finite element method) were used to find Γ_m and f_m, while the finite-difference time-domain (FDTD) method was used to calculate the total spontaneous emission rate Γ. These quantities allowed us to determine the total fiber-collected PL efficiency (η_{PL}) and individual supermode contributions $\eta_{\mathrm{PL},m}$. In addition, FDTD was used to obtain η_{PL} without use of supermodes.

Varying the channel width W_{ch} between 190 nm and 350 nm allows for significant modification of the supermode effective index n_{eff} . The real part of n_{eff} for the $\mathrm{hE}_{11}^{\mathrm{x}}$ doublet available

in this range, labeled I and II, is shown in Fig. 2(a). Both supermodes are guided, with $\text{Im}\{n_{\text{eff}}\} \approx 10^{-11}$. Field profiles for $W_{\text{ch}} = 190\,\text{nm}$ are shown in Fig. 1(b). Phase-matching between the fiber and E_{11}^x modes is apparent near $W_{\text{channel}} = 220\,\text{nm}$, where $f_{\text{I,II}}$ in Fig. 2(b) are equal. As W_{ch} increases, supermode $\text{hE}_{11}^{x,\text{I}}$ concentrates in the channel, resulting in reduced f_{I} and increased γ_{I} (Fig. 2(c)). Note, for $W_{\text{ch}} \gtrsim 240\,\text{nm}$, γ_{I} approaches the upper limit of 0.5. For z-oriented dipoles, two guided ($\text{Im}\{n_{\text{eff}}\} \approx 10^{-11}$) hE_{11}^y supermodes are available, labeled I and III, with $\text{Re}\{n_{\text{eff}}\}$ and $f_{\text{I,III}}$ plotted in Fig. 2(e)-(f). A third supermode, (leaky, $\text{Im}\{n_{\text{eff}}\} \gtrsim 10^{-7}$), $\text{hE}_{11}^{y,\text{II}}$, has the highest emission rate, though small f_{II}. Since the y-electric field component is dominant, γ_m for z-dipoles (Fig. 2(e)) is small compared to the x-dipole case. The highest contribution to η_{PL} is from the $\text{hE}_{11}^{x,\text{I}}$ supermode, with $\gamma_{\text{I}} \lesssim 0.04$.

Figure 3 shows total collection efficiency η_{PL} for x- and z-oriented dipoles (including emission in both $\pm z$ direcions, which is experimentally realizable), obtained with FDTD and the supermode expansion method of [11]. Since in each case multiple supermodes with differing propagation constants are excited, the collection efficiency oscillates along z, evidence of the power exchange between channel WG and fiber. Collection maxima for $1\,\mu\text{m} < z < 5\,\mu\text{m}$ are plotted for each W_{ch}. The collection efficiency for x-dipoles is maximized, nearing 70 %, for $W_{\text{ch}} \approx 220\,\text{nm}$. Near the optimal point, most ($\gtrsim 73$ %) of the emitted power is coupled into $\pm z$ propagating supermodes; fiber and slab are phase-matched, with equal fiber fractions of 50 %, so the $\eta_{\text{PL,I,II}}$ collection contributions are maximized. For z-dipoles, a more modest η_{PL} is achieved, due to lower γ_m and f_m (Figs. 2(f) and (g)). For $W_{\text{ch}} = 300\,\text{nm}$, η_{PL} reaches ≈ 25 % , however the total rate Γ is only ≈ 40 % of that in the x-dipole case.

We next show that the transmission through this directional coupler can be significantly affected by the presence of the embedded dipole. Dipole-mediated control of light transmission has been considered in studies involving free-space [2,6,7] and guided mode excitation [3–5], and also in cavity QED (e.g., [1, 13]). We start by describing spontaneous emission as an electric dipole-type interaction between the emitter and a vacuum field reservoir, given in terms of the coupler supermodes [2, 11, 15]. With the input-output formalism of [2], under the Markoff approximation, we obtain the following steady-state, positive-frequency, output multimode field operator for $z > z_0$ (i.e., past the dipole location):

$$\mathbf{E}^{(+)}(z,t) = i\sqrt{2\pi} \sum_m \sqrt{\frac{\hbar\omega}{4\pi S_m}} \mathbf{e}_m e^{-i(\omega t - \beta_m z)} \times$$
$$\times \left[\hat{a}_{in}^m(t - n_m z/c) + \sqrt{\Gamma_m}^* \sigma_-(t - n_m z/c) \right]. \tag{1}$$

Here, σ_- is the atomic lowering operator, $\hat{a}_{in}^m$ is supermode m's input field annihilation operator, $\mathbf{e}_m$ is the electric field distribution, β_m the propagation constant, n_m the phase index, and $S_m = \text{Re}\{\int_S dS(\mathbf{e}_m \times \mathbf{h}_m^*) \cdot \mathbf{z}\}$, with S the xy plane. The expression in brackets is a well-known result of the input-output formalism, with explicit input (or "free") field

and radiated ("source") field contributions [2]. Next, we assume the percentages of incident fiber mode power transferred to coupler supermodes at $z = 0$ are given by the fiber-mode fractions f_m, and that the power coupled into the output fiber at $z = L_c$ is approximated by an overlap integral between the field at this position and the fiber mode (Eq. (2) in [11]). This expression is translated into the fiber power operator

$$\hat{F} = \left\{ \int_S dS(\mathbf{E}^{(-)} \times \mathbf{h}_f) \cdot \mathbf{z} \int_S dS(\mathbf{e}_f^* \times \mathbf{H}^{(+)}) \cdot \mathbf{z} + \right.$$
$$\left. \int_S dS(\mathbf{H}^{(-)} \times \mathbf{e}_f^*) \cdot \mathbf{z} \int_S dS(\mathbf{h}_f^* \times \mathbf{E}^{(+)}) \cdot \mathbf{z} \right\} S_f^{-1}, \tag{2}$$

where $\mathbf{e}_f$ and $\mathbf{h}_f$ are the fiber mode electric and magnetic field distributions, and $S_f = \text{Re}\{\int_S dS(\mathbf{e}_f \times \mathbf{h}_f^*) \cdot \mathbf{z}\}$. Photon flux and higher order correlation functions at the output fiber may be obtained with $\hat{F}$. Using Eq. (1) into Eq. (2) and assuming a coherent state illumination source, an expression for the output fiber photon flux expectation value is obtained in the low-excitation limit (far below saturation), and normalized to the input photon flux F_{in} to produce the transmission level $F = \langle \hat{F} \rangle / F_{\text{in}}$. The resulting F expression consists of a sum of terms proportional to $f_m f_{m'}^* e^{i(\beta_m - \beta_{m'})(z - z_0)}$, and is used to calculate the transmission contrast through the fiber, defined as $\Delta T = (F - F_0)/F_0$, where F and F_0 are the transmission levels on and off resonance with an x-polarized dipole. The transmission contrast is significant over a bandwidth of the order of the transition linewidth (the Purcell enhancement is small in these structures), which is much smaller than the coupler transmission bandwidth. In Fig. 4, we plot F_0, F, and ΔT for a coupler with $W_{\text{ch}} = 220\,\text{nm}$ (phase-matched channel and fiber WGs). As expected for a directional coupler, F_0 oscillates along z between close to zero and close to unity, with beat length $L_\pi = \pi/(\beta_{\text{I}} - \beta_{\text{II}}) \approx 3.3\,\mu\text{m}$. The coupler 3 dB transmission bandwidth is $> 100\,\text{nm}$ for $L_c \lesssim 5\,\mu\text{m}$. For a dipole located at $z_0 = L_\pi/2$, F can be significantly enhanced or suppressed relative to F_0, depending on z: at $z - z_0 \approx 1.65\,\mu\text{m}$ ($L_\pi/2$), $F \approx 20\,\%$ is nearly 30 times larger than $F_0 < 1\,\%$; at $z - z_0 \approx 5.0$ μm, $F \approx 40\,\%$ is 2.4 times smaller than $F_0 \approx 96\,\%$. A judicious choice of coupler length L_c thus produces structures in which a single dipole strongly affects transmission. This could enable, e.g., measurements of emitter spectral diffusion, or, with AC or DC Stark effect emitter frequency control, dipole-controlled light modulation. We note that phase matching is crucial in such devices, as ΔT is limited by incomplete power transfer in phase-mismatched fiber and channel WGs. Figure 4(b) shows more modest results for $W_{\text{ch}} = 300\,\text{nm}$, due to phase mismatch ($\Delta T \approx -20\,\%$ may still be achieved).

If a single coupler supermode is accessed by the fiber, i.e., $f_m = 0$ for all but one supermode, we find $F = f_m^2 [1 - 4\gamma_m(1 - \gamma_m)]$, which illustrates the essential role of γ_m in extinction measurements [2]. Perfect extinction is predicted for $\gamma_m = 0.5$, or exclusive m-supermode emission. As emission is in both directions, this is equivalent to perfect reflection [7]. In

Fig. 2(c), it is apparent that extinction near 100 % may be achieved for $W_{\mathrm{ch}} > 250\,\mathrm{nm}$, provided only supermode $\mathrm{hE}_{11}^{x,I}$ is accessible. This situation can be approximated with WG mode conversion structures (e.g., lateral or vertical tapers) that favor coupling between the fiber mode and specific coupler supermodes [12]. For example, for $W_{\mathrm{ch}} = 300\,\mathrm{nm}$, a modest 80:20 coupling ratio to the type I and II supermodes (i.e., $f_{\mathrm{I}} = 0.8$, $f_{\mathrm{II}} = 0.2$, $f_{m\neq\mathrm{I,II}} = 0$) would lead to > 88 % extinction, independent of dipole position and coupler length.

In summary, we have investigated a hybrid waveguide structure in which strong dipole excitation is combined with efficient optical access through an evanescently-coupled optical fiber-based waveguide. These devices may have application in areas such as quantum information processing and single emitter spectroscopy.

References

1. H. J. Kimble, "Strong interactions of single atoms and photons in cavity QED," Physica Scripta **T76**, 127–137 (1998).
2. S. J. van Enk, "Atoms, dipole waves, and strongly focused light beams," Phys. Rev. A **69**, 043 813 (2004).
3. P. Domokos, P. Horak, and H. Ritsch, "Quantum description of light-pulse scattering on a single atom in waveguides," Phys. Rev. A **65**, 033 832 (2002).
4. J. T. Shen and S. Fan, "Coherent photon transport from spontaneous emission in one-dimensional waveguides," Opt. Lett. **30**, 2001–2003 (2005).
   http://ol.osa.org/abstract.cfm?URI=ol-30-15-2001
5. D. E. Chang, A. S. Srensen, E. A. Demler, and M. D. Lukin, "A single-photon transistor using nanoscale surface plasmons," Nature **3**, 807–812 (2007).
6. B. D. Gerardot, S. Seidl, P. A. Dalgarno, R. J. Warburton, M. Kroner, K. Karrai, A. Badolato, and P. M. Petroff, "Contrast in transmission spectroscopy of a single quantum dot," Appl. Phys. Lett. **90**, 221 106 (2007).
7. G. Zumofen, N. M. Mojarad, V. Sandoghdar, and M. Agio, "Perfect Reflection of Light by an Oscillating Dipole," Phys. Rev. Lett. **101**, 180 404 (2008).
   http://link.aps.org/abstract/PRL/v101/e180404
8. V. S. C. M. Rao and S. Hughes, "Single quantum-dot Purcell factor and beta factor in a photonic crystal waveguide," Phys. Rev. B **75**, 205 437 (2007).
   http://link.aps.org/abstract/PRB/v75/e205437
9. G. Lecamp, P. Lalanne, and J. P. Hugonin, "Very Large Spontaneous-Emission beta Factors in Photonic-Crystal Waveguides," Phys. Rev. Lett. **99** (2007).
10. Resonant fluorescence can also be studied, for example, through emission into the backward traveling WG mode.

11. M. I. Davanço and K. Srinivasan, "Efficient spectroscopy of single embedded emitters using optical fiber taper waveguides," Opt. Express **17**, 10542–10563 (2009). http://www.opticsexpress.org/abstract.cfm?URI=oe-17-13-10542

12. W.-P. Huang, "Coupled-mode theory for optical waveguides: and overview," J. Opt. Soc. Am. A **11**, 963–983 (1994).

13. K. Srinivasan and O. Painter, "Linear and nonlinear optical spectroscopy of a strongly coupled microdisk-quantum dot system," Nature (London) **450**, 862–865 (2007).

14. Far from cutoff, channel WG $E_{pq}^{x,y}$ modes are predominantly x- or y-polarized, with p and q maxima in the x- and y-directions respectively.

15. F. Le Kien, S. Dutta Gupta, V. I. Balykin, and K. Hakuta, "Spontaneous emission of a cesium atom near a nanofiber: Efficient coupling of light to guided modes," Phys. Rev. A **72**, 032 509 (2005).
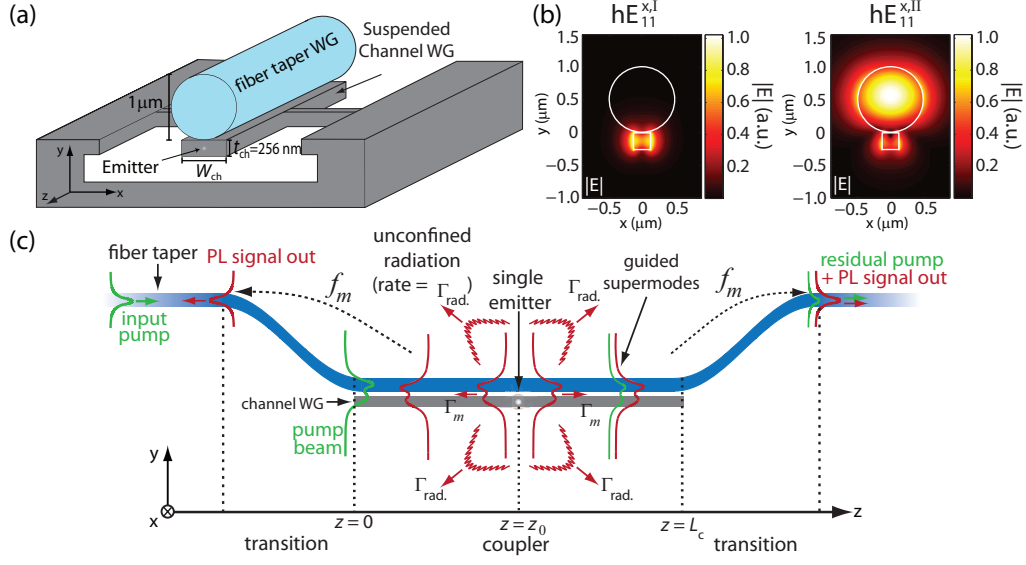
List of Figures

Fig. 1 Fiber taper/channel WG directional coupler scheme. (a) 3D schematic and coupler cross-section. (b) Hybrid $hE_{11}^{x,I}$ and $hE_{11}^{x,II}$ coupler supermodes for $W_{ch} = 190\,\mathrm{nm}$ and $\lambda = 1.3\,\mu\mathrm{m}$. (c) Non-resonant single dipole PL collection configuration.
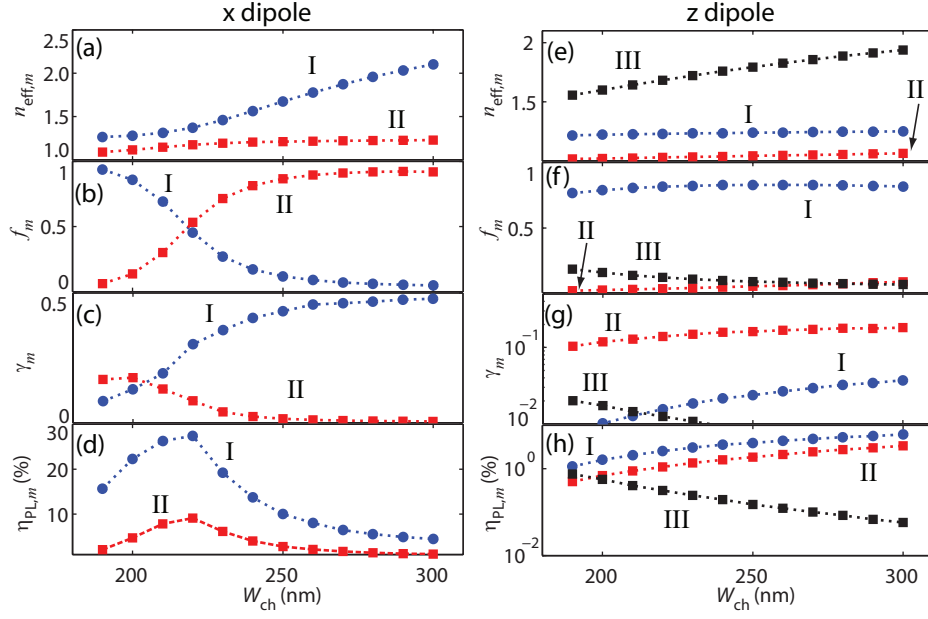
Fig. 2 Effective index $n_{\mathrm{eff},m}$, fiber mode fraction f_m, β-factor γ_m, and PL collection contribution $\eta_{\mathrm{PL},m}$ as functions of channel WG width W_{ch} for (a)-(d) $hE_{11}^{x,m}$ ($m = I$ or II) (e)-(h) $hE_{11}^{y,m}$ supermodes ($m = I$, II, or III).

Fig. 3 Maximum spontaneous emission collection efficiencies for (a) x- and (b) z-polarized dipole moments, as function of W_{ch}, calculated with FDTD and supermode expansion.

Fig. 4 Normalized, off- and on-resonance transmission (F_0 and F) and contrast $\Delta T = (F - F_0)/F_0$ as functions of separation from a single dipole at z_0, for (a) $W_{ch} = 220\,\mathrm{nm}$ and (b) $W_{ch} = 300\,\mathrm{nm}$.

Fig. 1. Fiber taper/channel WG directional coupler scheme. (a) 3D schematic and coupler cross-section. (b) Hybrid $\mathrm{hE}_{11}^{x,\mathrm{I}}$ and $\mathrm{hE}_{11}^{x,\mathrm{II}}$ coupler supermodes for $W_{\mathrm{ch}} = 190\,\mathrm{nm}$ and $\lambda = 1.3\,\mu\mathrm{m}$. (c) Non-resonant single dipole PL collection configuration.

Fig. 2. Effective index $n_{\mathrm{eff},m}$, fiber mode fraction f_m, β-factor γ_m, and PL collection contribution $\eta_{\mathrm{PL},m}$ as functions of channel WG width W_{ch} for (a)-(d) $\mathrm{hE}_{11}^{x,m}$ ($m = $ I or II) (e)-(h) $\mathrm{hE}_{11}^{y,m}$ supermodes ($m = $ I, II, or III).
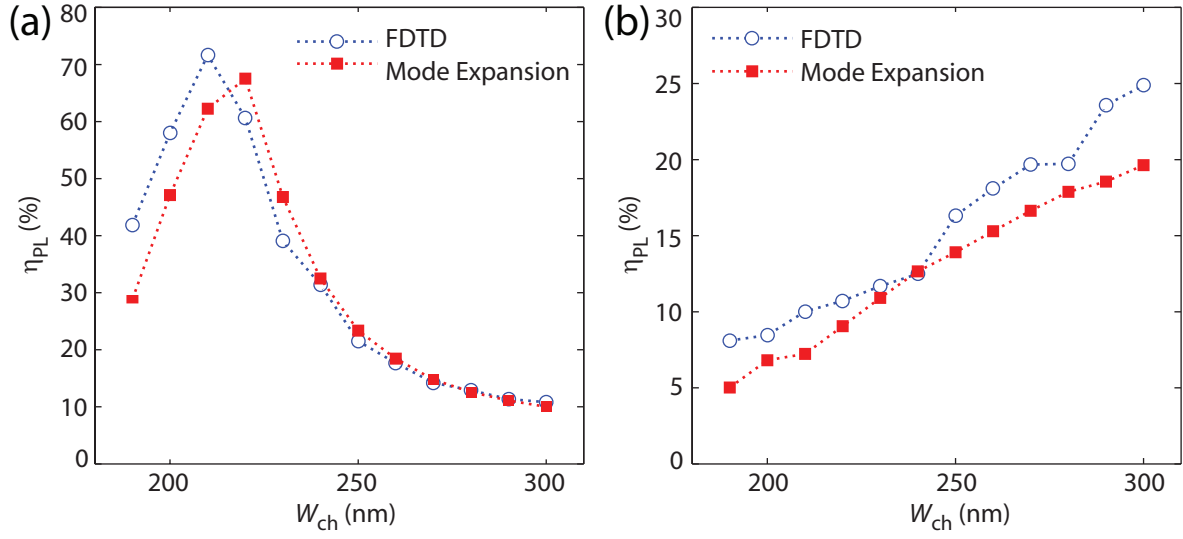
Fig. 3. Maximum spontaneous emission collection efficiencies for (a) x- and (b) z-polarized dipole moments, as function of W_{ch}, calculated with FDTD and supermode expansion.
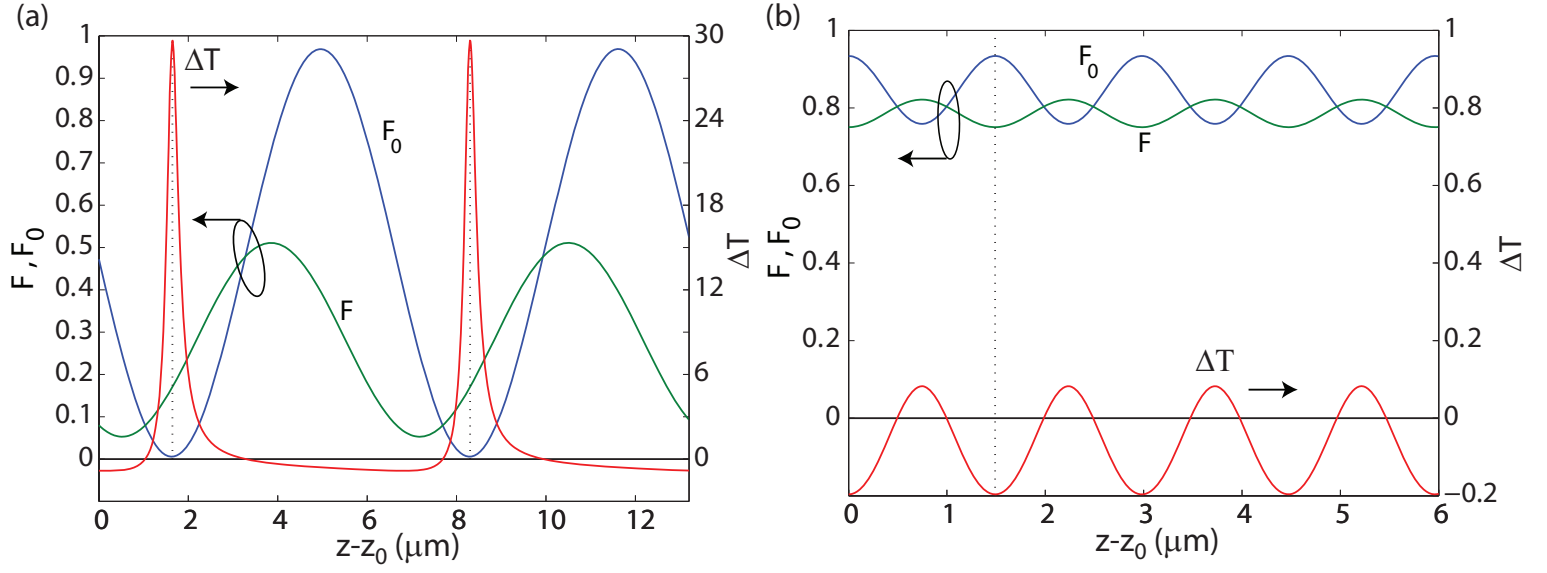
Fig. 4. Normalized, off- and on-resonance transmission (F_0 and F) and contrast $\Delta T = (F - F_0)/F_0$ as functions of separation from a single dipole at z_0, for (a) $W_{ch} = 220\,\text{nm}$ and (b) $W_{ch} = 300\,\text{nm}$.